MODELLING AND CHARACTERISATION OF BAINITE AND RETAINED AUSTENITE IN HOT ROLLED TRIP STEEL

SUWANPINIJ Piyada[1], LI Xiaoxiao[2], PRAHL Ulrich[2], BLECK Wolfgang[2]

[1]The Sirindhorn International Thai-German Graduate School of Engineering (TGGS), King Mongkut's University of Technology North Bangkok (KMUTNB), Thailand, piyada.s.mme@tggs-bangkok.org
[2]Department of Ferrous Metallurgy, RWTH Aachen University, Germany, EU

Abstract

A hot rolled TRIP steel was selected for the laboratory scale process simulation. The ferrite and bainite transformation kinetics on the run out table and during coiling were mapped as a function of temperature and austenite conditioning by Leblond and Devaux's concept. The updated carbon content in the remaining austenite is the key factor to control following bainite formation.

The microstructure was characterized by LOM, SEM, FEG EPMA. The mean carbon content was taken from the in-situ high energy XRD. Proper process window or austenite conditioning can be predicted for the required fractions of phases. Enough carbon enrichment of austenite can be achieved by forming carbide free bainite alone without the formation of ferrite at higher temperature. However, its fraction can be too low to exhibit the TRIP effect. Therefore, pre-deformation such that in the hot rolling process is still necessary.

Keywords: Bainite, TRIP steel, modelling, characterisation

## 1.	INTRODUCTION

This paper demonstrates how a simple numerical model described by a system of ordinary differential equations (ODEs) can help control complicated stepwise thermomechanical process to predict the process window in order to achieve the desired microstructure. The work extends the application of the rate law concept proposed by Leblond and Devaux [1] on dual phase (DP) steel, i.e., for ferrite and martensite, into transformation induced plasticity (TRIP) steel, i.e., for ferrite, bainite and consequently retained austenite (RA).

The adoption of the TRIP effect in the low alloy multiphase steels brings remarkable high energy absorption during crash, especially at higher strain rates. TRIP steel is generally composed of 50-70% ferrite, 25-30 % carbide free bainite, 10-20 % retained austenite and little martensite. The TRIP effect is mainly controlled by the amount of RA and its carbon content, which is controlled by carbon partitioning during preceding phase transformation. Bainite consists of sheaves of bainitic ferrite, and carbon-rich phases such as carbide, martensite and RA. The carbide free bainite is formed due to the suppression of carbide formation elements such as silicon and aluminium. The hot rolling process of TRIP steel follows the route shown in **Figure 1,** in which that of DP steel is compared. TRIP steel requires longer transformation time to form bainite during coiling. Meanwhile, carbon is partitioned into the remaining austenite continuously. This work takes the existing measured data from the in-situ synchrotron X-ray diffraction published earlier [2] for the modelling of bainite transformation. The bainitic ferrite fraction and carbon content in the remaining austenite were recorded at every 3 - 4 s.

## 2.	EXPERIMENTAL WORK

A TRIP steel with the chemical composition of (wt. %): 0.22C, 0.16Si, 1.65Mn, 1.25Al, 0.035Cr, 0.002Mo was selected. All the simulated hot rolling experiments were carried out in the deformation dilatometer Bähr DIL 805A/D and examined for phase fraction both in-situ and ex-situ. The cycles are shown in **Figure 2** and the

parameters are listed in **Table 1**. The in-situ investigation by synchrotron XRD follows the dashed cycle and the process parameters listed separately.
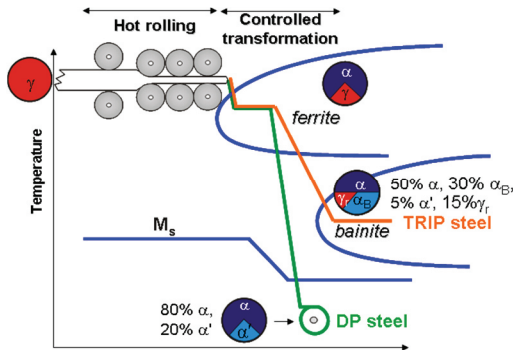

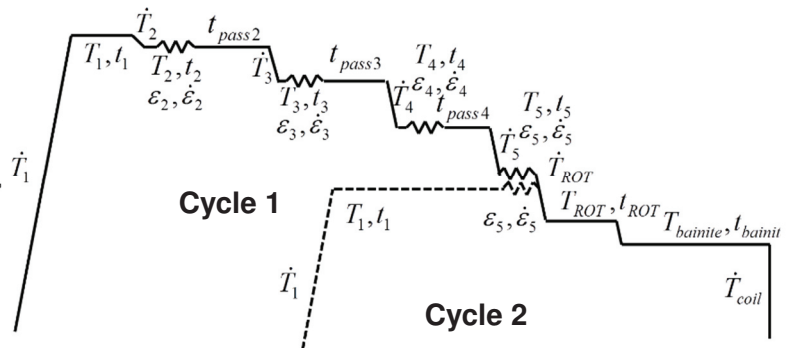**Figure 1** Schematic hot rolling route of TRIP and DP steels

Figure 2 The simulated hot rolling cycle

The metallographical work was performed by the best care as the deformation during grinding and polishing can transform some RA into martensite. Different etchants such as Klemm and Le Pera help differentiate different phases. Although ferrite and bainite are difficult to be differentiated, the ferrite and bainite formation temperatures were obviously different and the two phases with clearly different morphologies and location are expected. Scanning Electron Microscopy (SEM) is of use for the investigation of bainite.

Table 1 The experimental parameters in the shown in **Figure 2**. The underlined values are for the in-situ tests.

	$\dot{T}_1, T_1, t_1$	$\varepsilon_0, \dot{\varepsilon}_0$	$\dot{T}_2, T_2, t_2$	$\varepsilon_2, \dot{\varepsilon}_2$	$\dot{T}_3, T_3, t_3$	$\varepsilon_3, \dot{\varepsilon}_3$	$\dot{T}_4, T_4, t_4$
1	200 °C/min; 1250 °C; 900 s	-	4.3 °C/s; 1200 °C; 3 s	0.2; 5 s^{-1}	15 °C/s; 1150 °C; 3 s	0.4; 12 s^{-1}	30 °C/s; 1100 °C; 3 s
2	200 °C/min; 1000/1050 / 1100/1150/1200/1250 °C; 120, 300, 600, 900 s	0.0, 0.6, 1.2/12 s^{-1}	-	-	-	-	-

	$\dot{T}_1, T_1, t_1$	$\varepsilon_4, \dot{\varepsilon}_4$	$\dot{T}_5, T_5, t_5$	$\varepsilon_5, \dot{\varepsilon}_5$	$\dot{T}_{ROT}, T_{ROT}, t_{ROT}$	$\dot{T}_{bai}, T_{bai}, t_{bai}$	$\dot{T}_{RT}$
1	200 °C/min; 1250 C; 900 s	0.3; 12 s^{-1}	50 °C/s; 1050 °C; 3 s	0.0-0.3; 12 s^{-1}	60 °C/s; 600-780°C; 0-100 s	60 °C/s; 350-500 °C; 0-300 s	60 °C/s
2	200 °C/min; 1000/1050 / 1100/1150/1200/1250 °C; 120, 300, 600, 900 s	-	-	-	60 °C/s; 600-780 (660) °C; 0-100 (30) s	60 °C /s; 375, 400, 425, 450, 475, 500 °C;	60 °C/s

3.   EXPERIMENTAL RESULTS

The ferrite formed at higher isothermal step is obviously polygonal, mostly idomorph and some allotriomorph, and in some samples it clearly decorates the prior austenite grain boundaries as illustrated in **Figure 3(a)**. The transformation is fast at the beginning and saturates slowly. The bainitic ferrite forms inside the austenite grains, where carbon is enriched. Between the sheaf of bainitic ferrite, film-like RA is found. Under pre-deformation, the bainite is formed in smaller colonies as can be seen in **Figure 3(b)** as more polygonal ferrite is formed in larger fraction and is more homogeneously distributed. The RA is stable at the rim of the high carbon constituent while in the middle where the brownish colour appears indicates martensite. This has been

differentiated obviously by Klemm etchant such as in **Figure 3(b)**. The martensite can be formed also during the thermal cycle during the sample preparation. The latter micrograph is shown in a lower magnification to realise the amount of martensite on the surface.

Figure 3(c) and **3(d)** visualise clearer bainite structure when the isothermal transformation time increases from 20 s to 300 s. **Figure 3(c)** represents case without pre-deformation and **3(d)** is with a strain of 0.6 under which the bainitic constituent forms in smaller colonies. In contrary to **Figure 3(b)**, the RA shows much higher stability as much less brownish martensite can be observed in the micrograph. Also, the film-like RA becomes thinner but shows clearer sharp ridge. It has to be noted that the RA here is not considered as the second component of bainite which contains high carbon content but it is measured for a separated phase. The phase fraction of bainite in this work is therefore only the bainitic ferrite fraction.
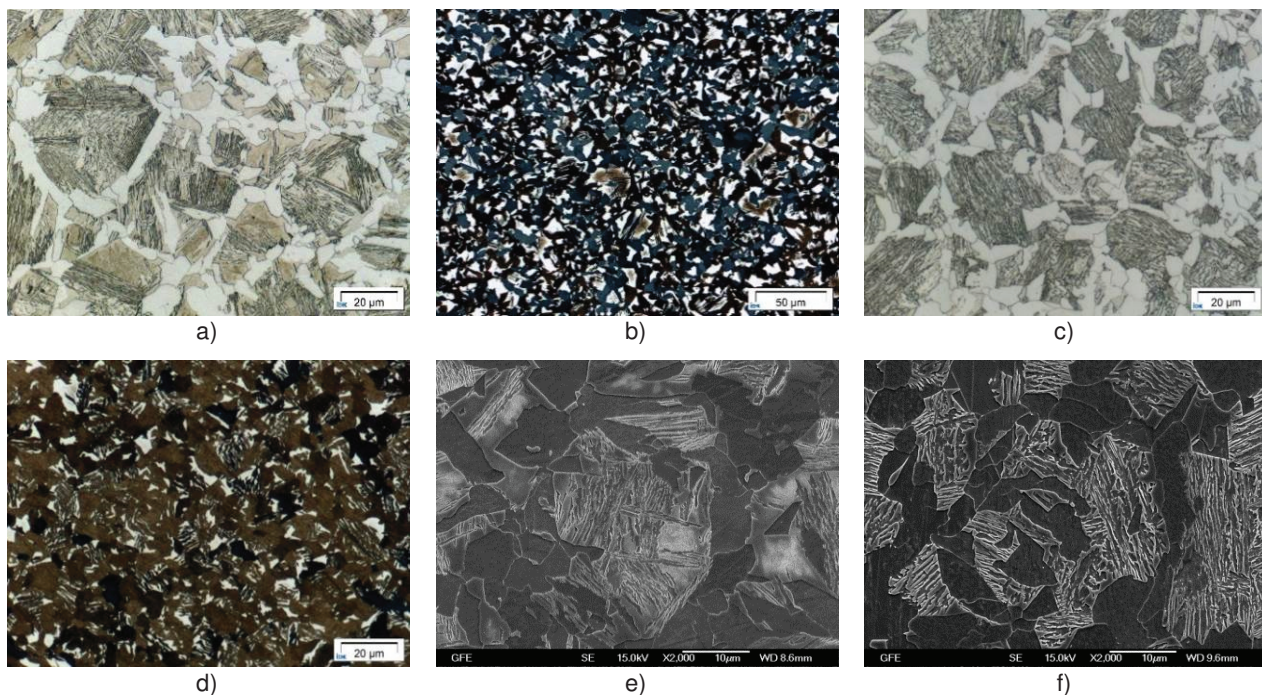

Figure 3 The microstructure of one-pass experiment under different parameters during bainite formation (a),(e) ε_5 = 0.0, $t_{bainite}$ = 20 s, nital (b) ε_5 = 0.6, $t_{bainite}$ = 20 s, Klemm (c),(f) ε_5 = 0.0, $t_{bainite}$ = 300 s, nital (d) ε_5 = 0.6, $t_{bainite}$ = 300 s, Klemm; For all, T_{ROT} = 660 °C, t_{ROT} = 30 s

4.   MODELLING WORK

The volume fractions of ferrite and bainite will be denoted by f and b, respectively, while, T is the temperature with time derivative $\dot{T}$. With these notations, the formation of ferrite and bainite in TRIP steel can be described by a few different equations. The formation kinetics of ferrite is modelled by

$$\dot{f}(t) = \left[f_{eq} - f \right]_+ \cdot g_{f1}(T) \cdot g_{f2}(D_\gamma, \varepsilon) \qquad (1)$$

Temperature influences the ferrite formation kinetics in 2 aspects. Firstly, the maximum achievable ferrite fraction denoted as f_{eq} can be calculated by CALPHAD and is a function of temperature. Secondly, the term $g_{f1}(T)$ is a parameter function of temperature.

The effect of austenite conditioning in **Figure 1** is contained in the function $g_{f2}(D_\gamma, \varepsilon)$ as follows,

$$g_{f2}(D_\gamma, \varepsilon) = \alpha_1 S_v(D_\gamma, \varepsilon) + \alpha_2 \qquad (2)$$

Here α_1, α_2 are the parameters that have to be fitted with the experimental data. The function S_v describes the effect of austenite grain size and retained strain. Due to the difficulty in defining S_v by experiment as the prior austenite grain boundaries are severely obscured by bainitic transformation during quenching deformed samples, S_v was taken from the empirical equation from Kvackaj [3] as shown in Eq. (3).

$$S_V = 429 \frac{1}{D_\gamma e^\varepsilon} + 1571 \frac{e^\varepsilon}{D_\gamma} + \left[157.2\left(1 - e^{-\varepsilon}\right) - 59.47\right]_+ \text{ (mm}^{-1}) \tag{3}$$

Likewise, the bainite transformation rate can be described as

$$\dot{b} = \left[b_{max}\left(C_\gamma, T\right) - b\right] \cdot g_{biso}(T) \cdot g_{bcon}(\dot{T}) \cdot g_{bc}(C_\gamma) \tag{4}$$

The b_{max} is to be identified from CALPHAD method and is a function of: $\overline{X}$, the average carbon content in austenite before bainite forms, X_{T_0}, carbon content at T_0, the locus of maximum carbon content at the end of phase transformation, and, $X_{Ae1para}$, the para-equilibrium carbon content of the bainitic ferrite as proposed by [4]. It can be written as

$$b_{max} = \frac{X_{T_0} - \overline{X}}{X_{T_0} - X_{Ae1para}} . \tag{5}$$

The second parameter g_{biso} is the effect of isothermal temperature. The parameter function g_{bc} describes the effect of carbon content in the remaining austenite, which is progressively enriched as bainite grows. The instantaneous carbon content and the bainite fraction were taken from the recorded in-situ measurement in an earlier paper [2] and used for the calculation of the g_{bc} function. The g_{bcon} function is equal to one at isothermal transformation. Continuous case is calculated by taking small increments at each isothermal step.

5. MODELLING RESULTS

Different ferrite fraction contours are illustrated in **Figure 4(a) and (b)**. Each contour line represents the phase fraction. The first is a function of the equivalent austenite grain size and formation temperature with a transformation time of 30 s. The second is a function of a starting grain size of 38 micrometer under different retained strain, with formation temperature with a holding time of 10 s. So, if a fraction of 0.5 is aimed, the austenite grain size of 40 μm will match with the

a) with different equivalent austenite grain size and transformation time of 30 s

b) with an austenite grain size of 38 μm with a transformation time of 10 s

Figure 4 Contours of ferrite fraction as a function of transformation temperature and austenite conditioning

transformation at 670 °C for 30 s, or higher or lower temperature for smaller grain size. The second contour predicts the same fraction at the same temperature but after a short transformation of 10 s, when the starting
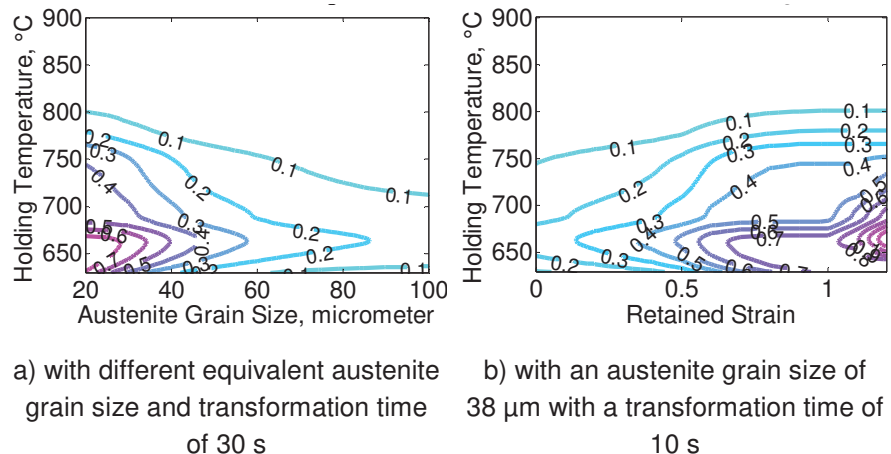
grain size of 38 μm is under a retained strain of 0.5. The austenite grain size at X-axis in **Figure 4(a)** means the austenite grain size which is inversely calculated from the relationship between S_v values from different austenite conditions in the function g_{f2} or namely "equivalent austenite grain size". The formation of enough fraction ferrite can be a requirement for good mechanical properties as well as for larger RA fraction as discussed in [2]. It is therefore useful to use the phase fraction contour of ferrite as guidance for proper process window.

During bainite transformation, the effect of temperature in the range 375 - 500 °C on its kinetics is stored in the function of g_{biso}. Regardless the transformation temperature, carbon content in the remaining austenite recorded by the in-situ measurement can be plotted nonlinearly along the increasing bainitic ferrite fraction as shown in **Figure 5.** The data was stored into the g_{bc} function and hence the bainite transformation can be mapped as a function of both temperature and carbon content in the austenite as shown in **Figure 6**.
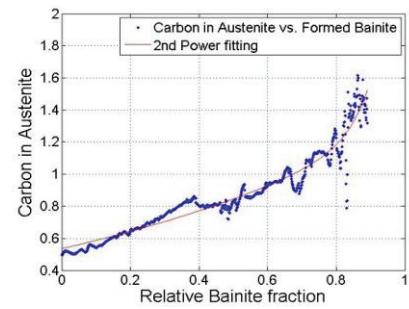

Figure 5 The collected data of carbon content in austenite obtained by a former in-situ XRD
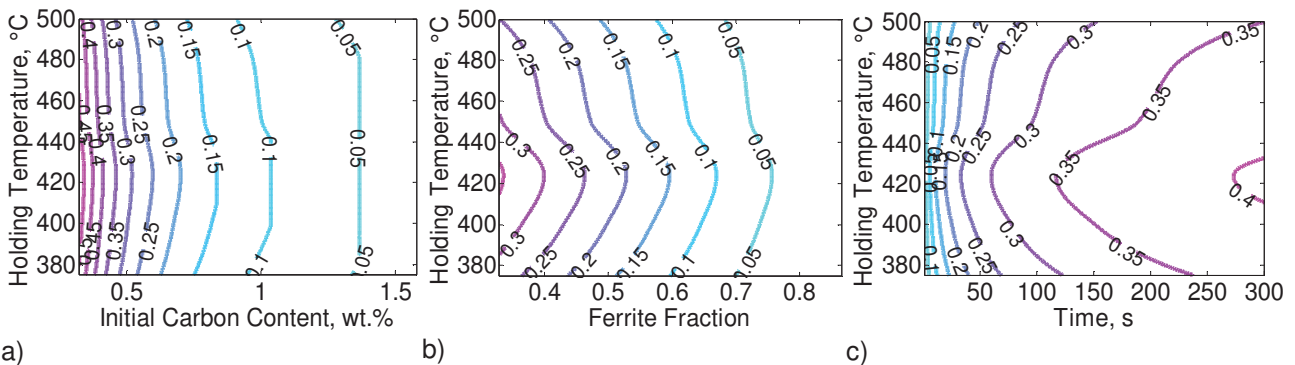

a)   b)   c)

Figure 6 Modelling results of bainite transformation a) at different initial carbon contents after a transformation time of 300 s. b) after different former ferrite fraction formed in 30 s. c) after different transformation time at a constant initial carbon content of 0.4 %

Figure 6(a) shows the phase fraction of bainite after different transformation periods as a function of the starting carbon content in austenite before bainite forms. Likewise, **Figure 6(b)** plots the effect of carbon content in austenite as the existing ferrite fraction formed at the higher temperature. Similarly, in case of a constant carbon content of 0.4 wt. % after the ferrite formation is shown in **Figure 6(c)**. It can be seen that the temperature around 430 °C allows fastest bainite formation.
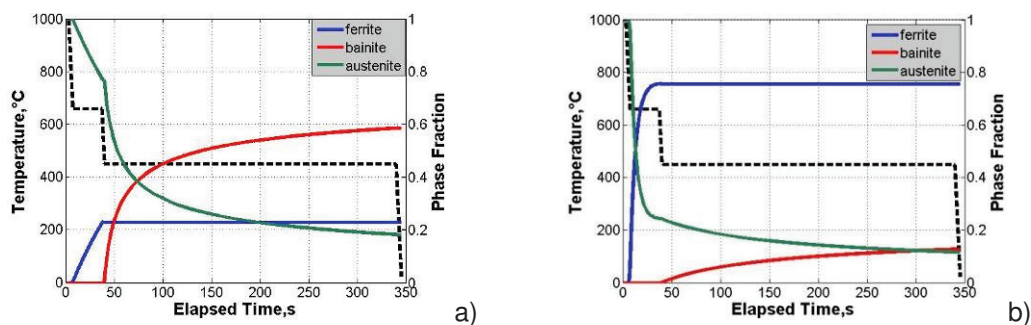

a)   b)

Figure 7 The development of phases by the models a) with an austenite grain size of 73 μm and no pre-deformation b)with an austenite grain size of 38 μm and a pre-deformation of 0.6

When combining the models for ferrite and bainite transformation, the development of phases along the simulated hot rolling process can be represented as in **Figure 7(a)** and **7(b)**. The first is the case of a large strain free austenite grain size of 73 μm followed by bainite formation at 450 °C for 300 s. The latter is from a smaller austenite grain size of 38 μm with a retained strain of 0.6. The shown fraction of the remaining austenite can be subtracted from the existing amount of ferrite and bainite. However, in case of instable austenite, large inner part of it transforms into martensite during cooling and results in much lower amount of RA. This is the matter of carbon distribution profile inside the remaining austenite. Smaller fraction of remaining austenite such as the one revealed in **Figure 7(b)** actually results in much more stable RA. The high energy XRD after cooling was used to prove for this and shows a higher fraction of 0.16 for the RA in this case. Without the pre-deformation, 5% less in RA is measured. The martensite transformation from unstable austenite still needs an extra model.

6.   DISCUSSION

A special feature of this work is the acquisition of in-situ carbon content along the growth of bainite. This allows the setup of more precise parameter function of carbon content a main controlling factor on bainite transformation kinetics. Plotting the bainite fraction with carbon content shows that much larger bainite fraction forms when carbon content in austenite is lower such as in case of little existing ferrite fraction. This corresponds to the result that sample without pre-deformation forms mostly bainite with insufficient ferrite as well as RA to be a TRIP steel.

The ex-situ data can be acquired by stepwise quenching for the microstructure and mass balance calculation for the carbon content and are still necessary as synchrotron beamtime is usually limited but quality of ex-situ data relies on the "freezing" effect of quenching. At the temperature region where transformation is fast, quenching can be ineffective as the phase still grows further. On the other hand, at the region where phase transformation is retarded, the transformation is stopped during quenching and more accurate data can be measured. This is one reason of some discontinuity in the results.

The model needs simple mathematics with numerous experimental data, between which the parameter functions are interpolated. Therefore, it can be used just for samples with small deviation in the chemical composition. However, simple differential equations allow fast calculation that on-line process optimization is possible [5]. This will be beneficial in terms of production of specific steel grade.

7.   CONCLUSIONS

The paper shows that the modelling results can be good guidance for setting the process parameters for thermomechanical process for the required microstructure. The pre-deformation in austenite before the ferrite formation is still helpful for the production of TRIP steel as it facilitates larger final RA fraction. Without the pre-deformation, small fraction of ferrite can be formed, resulting in low carbon content in the austenite and too large fraction of bainitic ferrite. Consequently, too little fraction is left for the RA. The in-situ measurement of carbon content by the synchrotron XRD is advantageous for the modelling of bainite transformation as bainite transformation period is relatively long after coiling and carbon content is increasing progressively and nonlinearly. Future work can include the evaluation of martensite formation from unstable austenite during cooling.

REFERENCES

[1]   LEBLOND, J. and DEVAUX, J. A. New Kinetic Model for Anisothermal Metallurgical Transformation in Steels including Effect of Austenite Grain Size. Acta Metal., 1984, vol. 32, pp. 137-146.

[2]   SUWANPINIJ, P., STARK, A., LI, X. RÖMER, F., HERRMANN, K. LIPPMANN, TH., BLECK, W. In-Situ High Energy X-Ray Diffraction for Investigating the Phase Transformation in Hot Rolled TRIP-Aided Steels. Advanced Engineering Materials, 2014, vol. 16, pp.1044-1051.

[3]   KVAČKAJ, T. and MAMUZIC, I. A. Quantitative Characterization of Austenite Microstructure after Deformation in Nonrecrystallization Region and its Influence on Ferrite Microstructure after Transformation. ISIJ Int., 1998, vol. 38, pp. 1270-1276.

[4]   TAKAHASHI, M. and BHADESHIA, H.K.D.H. A Model for Microstructure of some Advanced Bainitic Steels. Mater. Trans. JIM, 1991, vol. 32, pp. 689-696.

[5]   BLECK, W., HÖMBERG, D., PRAHL, U., SUWANPINIJ, P., TOGOBYTSKA, N. Optimal Control of a Cooling Line for Production of Hot Rolled Dual Phase Steel. Steel Research Int., 2014, 85, pp. 1328-1333.